ELSEVIER

Thermochimica Acta, 242 (1994) 173–186

thermochimica acta

Kinetic and mechanistic study of the non-isothermal decomposition of manganese(II) acetate tetrahydrate

M.A. Mohamed *, S.A. Halawy

Department of Chemistry, Faculty of Science, Qena, Egypt

(Received 20 October 1993; accepted 27 January 1994)

Abstract

The non-isothermal decomposition of manganese(II) acetate tetrahydrate was studied between ambient temperature and 500°C by means of thermogravimetry (TG), derivative thermogravimetry (DTG), differential thermal analysis (DTA) and differential scanning calorimetry (DSC). The dehydration process was found to take place in two consecutive steps. The first step commences early ($\approx$20°C) while the second step is accompanied by melting (at 120°C) with the evolution of acetic acid. Careful investigation of the course of the decomposition revealed that two reaction intermediates are formed. The first was identified as acetyl manganese acetate, $Mn(CH_3COO)_2 \cdot COCH_3$, at $\approx$120°C, which is believed to form during the second dehydration step. The second intermediate compound was identified as manganese acetate hydroxide, $Mn(CH_3COO)_2 \cdot OH$, formed near 155°C in an exothermic process. This is followed by the decomposition of the hydroxide intermediate to form MnO as a solid product, with possible melting. Then, catalytic decomposition of the anion takes place, with the formation of initial gaseous products on the surface of MnO. In air, however, Mn_3O_4 is formed as a residual solid product.

IR spectroscopy, X-ray diffractometry and scanning electron microscopy (SEM) were used to identify and investigate the solid decomposition products. Gas chromatography (GC) was used to identify the volatile gaseous products as acetone, acetic acid, CO, CO_2 and trace amounts of acetaldehyde. Methane and isobutene were formed at high temperatures, i.e. at 290°C.

The kinetic parameters (activation energy ΔE, and frequency factor $\ln A$), and the thermodynamic parameters (enthalpy change ΔH, heat capacity C_p, and the entropy change ΔS), were calculated for the dehydration and the decomposition processes.

Keywords: Atmosphere; Decomposition; DSC; DTA; GC; IRS; Kinetics; Manganese acetate; Mechanism; Non-isothermal; SEM; TG; Thermodynamics; XRD

* Corresponding author.

SSDI 0040-6031(94)01742-Y

1. Introduction

Over a number of years, metal carboxylates have been the subject of many studies in the field of the thermal decomposition of solids [1]. The majority of these studies have been concerned with the kinetics and the mechanisms of the decomposition of transition metal oxalates, e.g. copper [2], nickel [3] and iron [4, 5]. This can be attributed to the straightforward nature of the decomposition products of oxalates, where CO (or CO_2), or a mixture of the two, are the only gaseous products, and the corresponding metal, or metal oxide, is formed as the residual solid product.

The decomposition of metal acetates, has also received some attention because they are important precursors for the preparation of metal oxide catalysts [6].

A number of these acetates have been found to decompose via the formation, and consequent decomposition, of reaction intermediates. IR spectroscopy (gas phase and solid phase), gas chromatography, and X-ray diffraction techniques were used in these studies. For example, nickel acetate is reported [7, 8] to form a basic acetate salt, $Ni(CH_3COO)_2 \cdot Ni(OH)_2$, and nickel carbide, Ni_3C, as two reaction intermediates. Lead acetate is known [9, 10] to decompose via two different basic salts, $Pb(CH_3COO)_2 \cdot PbO$ and $Pb(CH_3COO)_2 \cdot 2PbO$.

In a recent study using IR and mass spectrometry [11], cobalt(II) acetate tetrahydrate was found to form two different intermediate compounds, acetyl cobalt acetate, $Co(CH_3COO)_2 \cdot COCH_3$, and cobalt acetate hydroxide, $Co(CH_3COO)_2 \cdot OH$.

The distribution of the volatile decomposition products of metal acetates was found to be influenced by the prevailing atmosphere [10]: acetic acid represents the major product in N_2 atmosphere while acetone predominates in the presence of oxygen [10]. In addition, some other volatile products have been reported [9, 12] from the decomposition of metal acetates, including CO_2, CO, methane, isobutene, acetaldehyde and ethyl acetate.

Manganese(II) acetate tetrahydrate, the subject of the present study, has been reported [13] as decomposing to form two different anhydrous salts with no reaction intermediates. MnO was identified as the solid product in N_2 atmosphere while Mn_2O_3 is produced in oxygen. Manganese(III) acetate is reported to form a basic acetate salt, $Mn(CH_3COO)_2 \cdot OH$, as a reaction intermediate [14].

The present article is intended to extend our previous work on the decomposition of transition metal acetates, namely those of nickel [8] and cobalt [11]. We have applied the available analytical techniques in order to identify the possible reaction intermediates accompanying the decomposition process. Scanning electron microscopy (SEM) was also used to investigate the possible occurrence of melting during the reaction. A comparison of the decomposition course, and the kinetic and thermodynamic parameters with those of similar systems is also given.

2. Experimental

2.1. Materials and techniques

The manganese(II) acetate tetrahydrate used in the present study was an analytical grade material (PROLABO, France), used with no further purification.

Thermogravimetry (TGA), derivative thermogravimetry (DTG), differential thermal analysis (DTA) and differential scanning calorimetry (DSC) were carried out using a Shimadzu 'stand-alone' thermal analyser (TGA-50H, DTA-50 and DSC-50), Japan. The analyser is equipped with a data acquisition and handling system (Chromatopac C-R4AD).

All thermal analysis experiments were performed in a dynamic atmosphere (40 ml min^{-1}) of N_2, H_2 or air. The parent salt was gently crushed before use to ensure particle size homogeneity. Comparable sample weights (10–15 mg) were always used to avoid the effect of variation of sample weight on the peak shape and peak temperature [15].

Highly sintered α-Al_2O_3 powder (Shimadzu) was used as a reference material for the DTA and DSC measurements. The heat of transition of pure indium metal (Johnson Matthey) at 157°C (28.24 J g^{-1} [16]) was adopted for the DSC calibration.

X-ray powder diffraction analysis (of the parent salt, its decomposition solid products and the solid residue under different atmospheres) was carried out by means of a Model JSX-60 PA Jeol diffractometer (Japan) equipped with a source of Ni-filtered Cu Kα radiation ($\lambda = 1.5405$ Å). Results were matched with ASTM standards.

The gas-phase decomposition products of anhydrous manganese acetate were analysed using a Shimadzu computerized gas chromatograph (Model GC-14 A). Dry N_2 (or dry O_2) was used as a dynamic atmosphere (85 ml min^{-1}) and as a carrier. Details of the GC system and technique are given elsewhere [10].

IR spectroscopy of the parent salt and its solid decomposition products was performed using a Model 1430 Perkin-Elmer ratio-recording IR spectrometer (between 4000 and 200 cm^{-1}).

Scanning electron microscopy (SEM) was used to investigate the parent salt and its solid decomposition products at different temperatures using a Model JSM T-2000 Jeol scanning electron microscope (Japan). The instrument was operated at low voltage (10–15 kV) to minimize specimen damage [17]. Before examination, samples were pre-coated with a thin film of Au/Pd.

2.2. Data analysis

Kinetic parameters, such as the activation energy ΔE (kJ mol^{-1}) and the frequency factor $\ln A$ (min^{-1}), were calculated for the dehydration and the decomposition processes using the Kissinger equation [18] and also the Coats–Redfern equation [19]. Details of the calculations are described elsewhere [10, 13].

The thermodynamic parameters, i.e. enthalpy change ΔH (kJ mol^{-1}), heat capacity C_p (kJ K^{-1} mol^{-1}) and entropy change ΔS (kJ K^{-1} mol^{-1}) for the dehydration and the decomposition processes were calculated as described elsewhere [10].

3. Results and discussion

3.1. Thermal analysis

3.1.1. Thermogravimetry (TG) and differential thermal analysis (DTA)

Figure 1 shows the TG, DTG and DTA curves of the decomposition of the parent manganese acetate tetrahydrate in N_2 atmosphere at 5°C min^{-1}. The TG curve shows two weight-loss steps. The first step takes place between 20 and 125°C and is accompanied by 29.25% weight loss. This step is attributed to the dehydration of the parent tetrahydrate to produce the anhydrous salt (theoretically, $4H_2O$ represents 29.4%). This step is followed by a small weight loss up to 190°C. The second weight-loss step takes place between 190 and 346°C and is associated with a weight loss of 40.66%. The total weight loss, after the complete decomposition, is measured from a number of experiments to be 70.5%. This suggests that the final residual solid product is MnO (theoretically, an MnO residue should result in a weight loss of 71%).

The DTG curve reveals that the dehydration process is composed of two overlapping steps with two maxima at 65.6 and 88.6°C. The decomposition also appears as a two-step process, two DTG maxima appearing at 323.2 and 338.1°C.

TG curves performed in H_2 atmosphere were broadly similar to those in N_2 except that the two DTG decomposition peaks were shifted towards lower temperatures, i.e. 309.5 and 327.9°C, compared to 323.2 and 338.1°C in N_2 atmosphere. The total weight loss calculated in H_2 (69.9%) was close to that measured in N_2 (70.5%). This suggests the formation of the same final solid residue, i.e. MnO, in both atmospheres. In oxygen, however, the total weight loss was less than the corresponding values calculated in H_2 or in N_2. This suggests that a different solid residue is produced in O_2.

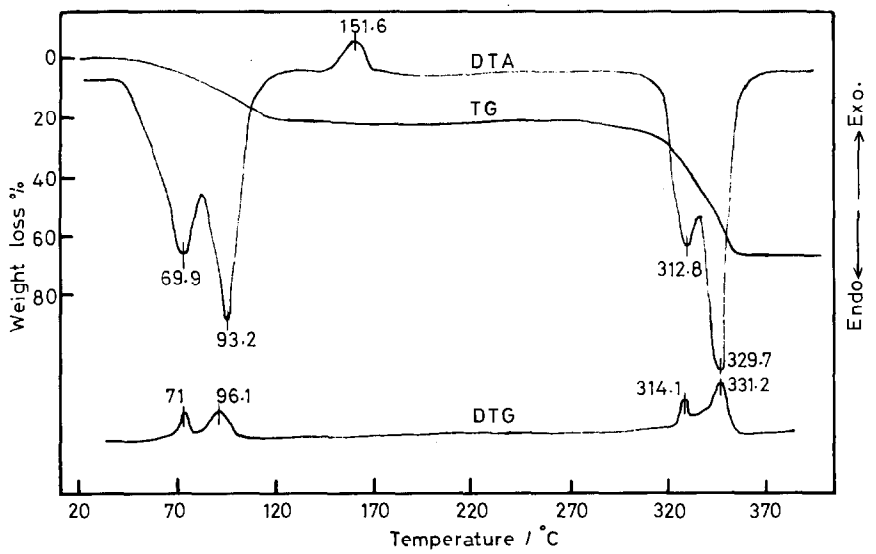

Fig. 1. TG, DTG and DTA curves for the decomposition of manganese acetate tetrahydrate at 5°C min^{-1} in N_2 atmosphere.

Table 1
Kinetic parameters of the dehydration and decomposition processes of manganese acetate tetrahydrate

Parameter	Calculated from	Peak I (endo)	Peak II (endo)	Peak III (exo)	Peak IV (endo)	Peak V (endo)
ΔE/(kJ mol^{-1})	DTA, Kissinger	102 ± 13	104 ± 2	161 ± 33	287 ± 47	414 ± 38
ln(A/min^{-1})		38 ± 5	36 ± 0.6	47 ± 9	61 ± 9	83 ± 5
ΔE/(kJ mol^{-1})	TG, Coats–Redfern	110 ± 12	87 ± 7	–	266 ± 35	392 ± 36
ln(A/min^{-1})	(ϕ = 3°C min^{-1})	40 ± 5	29 ± 3	–	59 ± 9	79 ± 5

The DTA curve, Fig. 1, displays five peaks which are labelled I–V. These are maximized at 60.2 (endo), 91.3 (endo), 154.5 (exo), 308.4 (endo) and 328°C (endo), respectively. Endotherms **I** and **II** are ascribed to the two dehydration steps, while endotherms **IV** and **V** are attributed to the two decomposition steps. Exotherm **III**, however, represents a process that is accompanied by no appreciable weight loss, see TG and DTG curves (Fig. 1).

The variation in the DTA peak temperatures with the rate of heating ϕ was used to calculate the activation energy ΔE (kJ mol^{-1}) and the frequency factor ln A (min^{-1}) for each process, using the Kissinger equation [18] with six different rates of heating. These kinetic parameters (ΔE and ln A) were also calculated from the TG data obtained at different heating rates using the Coats–Redfern equation [19]. Table 1 summarizes the kinetic parameters calculated using both methods.

The effect of using different dynamic atmospheres is shown in Fig. 2 which shows three DTA curves recorded at 10°C min^{-1} using N_2, H_2 and O_2 atmospheres (all experiments were performed at a flow rate of 40 ml min^{-1}). The DTA curve measured in H_2 is broadly similar to that in N_2, except that five peaks are slightly shifted towards lower temperatures. In an atmosphere of O_2, however, the first three peaks (I–III) are very similar to those in N_2 and H_2 atmospheres. Then a very strong, sharp exotherm appears, commencing at 253°C, instead of the two endothermic peaks (**IV** and **V**) seen in the N_2 and H_2 curves.

3.1.2. Differential scanning calorimetry (DSC)

Figure 3 shows two DSC curves for the decomposition of the parent salt at 5°C min^{-1}, one in N_2 and the other in H_2. In general, the DSC curves are very similar to the DTA curves in that four endotherms and one exotherm are observed. Again, the use of H_2 atmosphere results in no significant change in the shape and features of the DSC curve, which is similar to the DTA results.

DSC measurements were used to calculate the thermodynamic parameters, ΔH, C_p and ΔS, for the dehydration and decomposition processes as explained above. These values, calculated in N_2 and in H_2 atmospheres, are given in Table 2. The thermodynamic functions calculated in N_2 atmosphere are higher than those calculated in H_2. For example, the enthalpy change ΔH values in N_2 are three times those measured in H_2. This was found, experimentally, to be due to the nature of

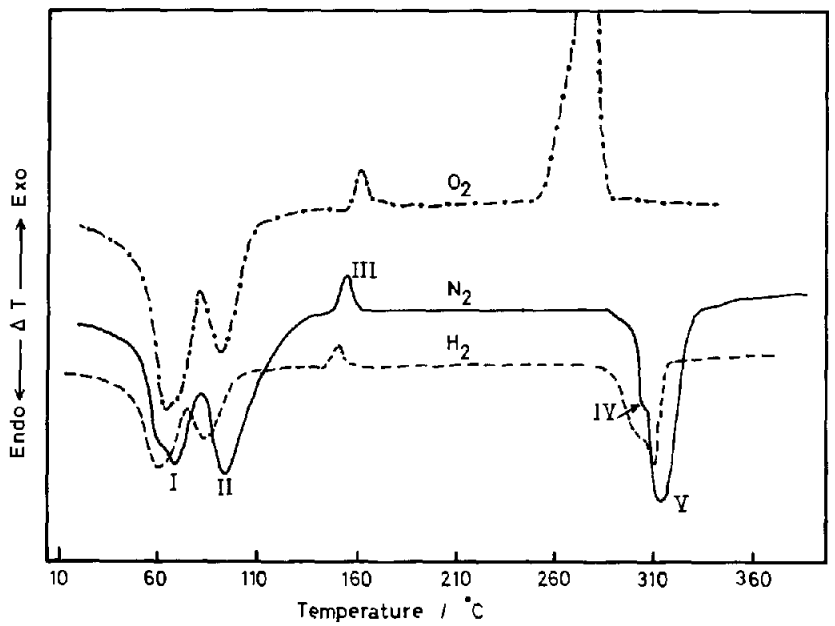

Fig. 2. The effect of atmosphere on the DTA curves (at 10°C min^{-1}): ——, in N_2; – – –, in H_2; and – · – · –, in O_2.

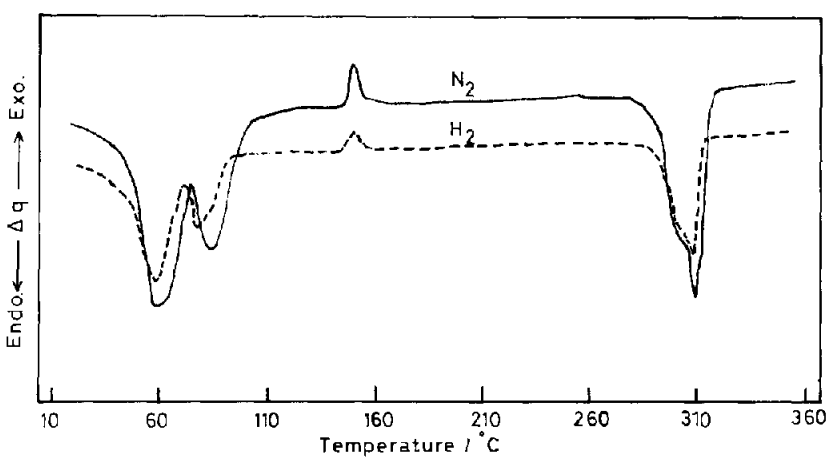

Fig. 3. The effect of atmosphere on the DSC curves (5°C min^{-1}): ——, in N_2; and – – –, in H_2.

H_2 and is not a result of any chemical change. To confirm this, the heat of transition ΔH of Specpure indium metal was calculated in N_2 and in H_2 atmospheres; it was found that the ΔH value in N_2 (23 J g^{-1}) was almost three times the corresponding value in H_2 (8.9 J g^{-1}).

Table 2
Thermodynamic parameters for the dehydration and decomposition processes of manganese acetate tetrahydrate in N_2 and H_2 atmospheres

Parameter	Atmosphere	Dehydration (I + II)	Process III	Decomposition (IV + V)
ΔH/(kJ mol^{-1})	N_2	162.5	6.9	81.4
C_p/(kJ K^{-1} mol^{-1})		1.89	0.46	1.83
ΔS/(kJ K^{-1} mol^{-1})		2.31	0.05	0.22
ΔH/(kJ mol^{-1})	H_2	56.5	−2.9	38.00
C_p/(kJ K^{-1} mol^{-1})		0.93	0.17	1.07
ΔS/(kJ K^{-1} mol^{-1})		1.13	−0.02	0.13

3.2. IR spectroscopy

Figure 4 shows five IR absorption spectra, between 4000 and 200 cm^{-1}, of the parent manganese acetate tetrahydrate (a) and its solid decomposition products in N_2 at different temperatures.

Spectrum (a) of the parent salt shows four absorption bands attributed to water of crystallization: 3500–3200 cm^{-1} (ν(OH)), 1640 cm^{-1} (δ(OH)) [10], 890 and 770 cm^{-1} [20]. A number of bands that are characteristic of the acetate anion [21, 22] appear at 1050 and 1030 cm^{-1} ($\rho(CH_3)$), 960 and 933 cm^{-1} (ν(C–C)), 670 cm^{-1} (δ(OCO)) and 614 cm^{-1} ($\pi(COO^-)$). Two other bands at 1578 and 1415 cm^{-1} are assigned to $\nu_{as}(COO^-)$ and $\nu_s(COO^-)$, respectively. The deformation modes of the CH_3 group are at 1442 cm^{-1} ($\delta_{as}(CH_3)$) and 1343 cm^{-1} ($\delta_s(CH_3)$) [21].

Spectrum (b), on heating parent salt at 125°C, shows two small sharp absorptions at 3030 and 2950 cm^{-1} which are ascribed to two different C–H stretching modes. These can be attributed to the presence of $COCH_3$ and CH_3 groups [21] respectively. Three of the characteristic bands of water of crystallization (at 1640, 890 and 770 cm^{-1}) have disappeared, while a broad band has appeared at 3450 cm^{-1} which can be attributed to the presence of OH group. An important feature is that the intensity of the absorption at 1343 cm^{-1} has decreased and a new sharp peak has appeared at 1316 cm^{-1}.

On heating at 150°C, the spectrum (c) is essentially similar to (b), at 125°C, except that the intensity of the new absorption peak at 1316 cm^{-1} has decreased, while the 1343 cm^{-1} peak has increased. This indicates the presence of two different methyl groups, i.e. CH_3 and CH_3CO.

Spectrum (d) (after heating at 260°C) shows a broad band at 3450 cm^{-1} which is characteristic of ν(OH), indicating the formation of a hydroxyl compound. The spectrum suggests the presence of two different COO^- groups (bands at 1650 and 1470 cm^{-1}, and at 1575 and 1405 cm^{-1}). The absorption band at 1316 cm^{-1} has completely disappeared while that at 1343 cm^{-1} is stronger. This can be attributed to the decomposition of the intermediate acetyl compound.

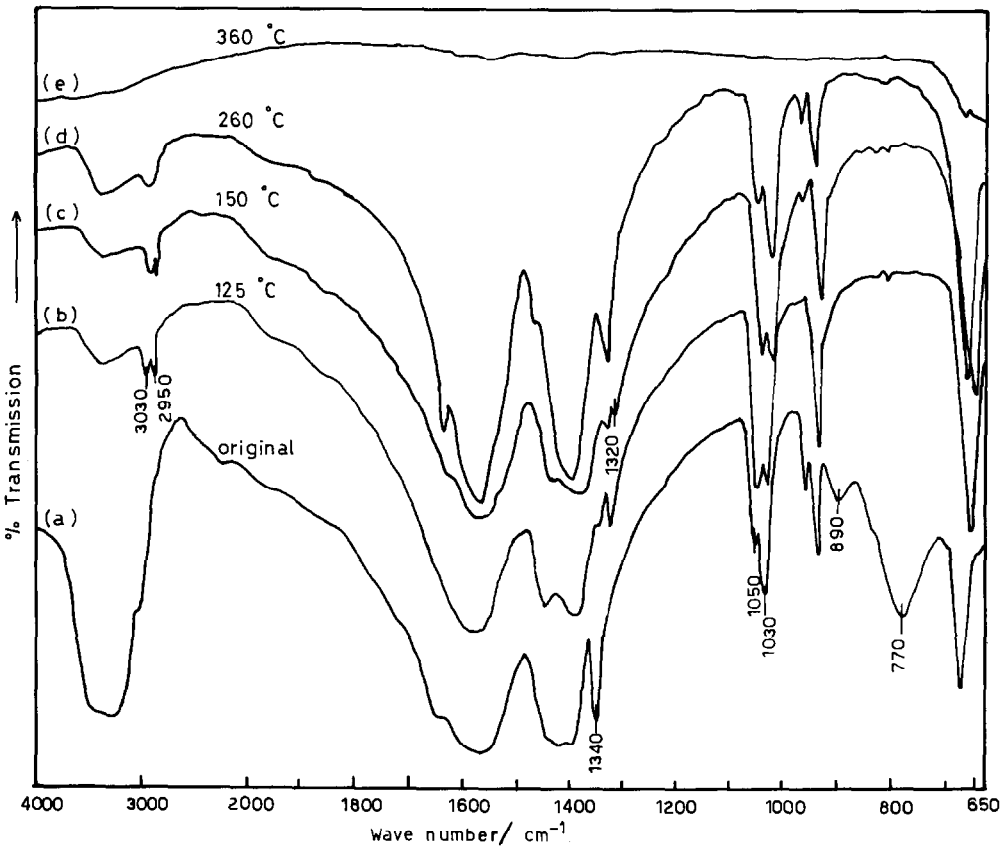

Fig. 4. IR spectra of the parent manganese acetate tetrahydrate (a) and its decomposition solid products at 125°C (b), 150°C (c), 260°C (d) and 360°C (e), all in N_2 atmosphere.

It should be mentioned here that the two absorption bands of CH_3 (at 1050 and 1030 cm^{-1}) have different intensities in the parent tetrahydrate salt (spectrum (a)). After the dehydration, these two peaks have equal intensity (spectra (b) and (c)). At 260°C (spectrum (d)), these two peaks regain their unequal intensities, as shown in the parent salt. This behaviour can be attributed to the coordination of an electron-donor group with the same effect as water molecules, and therefore they possess the same unequal intensities as the hydrated salt. This electron-donor group could be a hydroxyl group.

At 360°C (spectrum (e)), all absorption bands have disappeared, indicating complete decomposition of the acetate anions.

The IR spectra of the solid decomposition products on heating at 400°C under different atmospheres are shown in Fig. 5. In N_2 or H_2 atmospheres, the solid product (spectrum (a)) shows the characteristic absorptions of MnO [23] at 560, 462 and 345 cm^{-1}. In an O_2 atmosphere, however, the product shows the characteristic bands of Mn_3O_4 at 609, 494, 413 and 346 cm^{-1} [24].

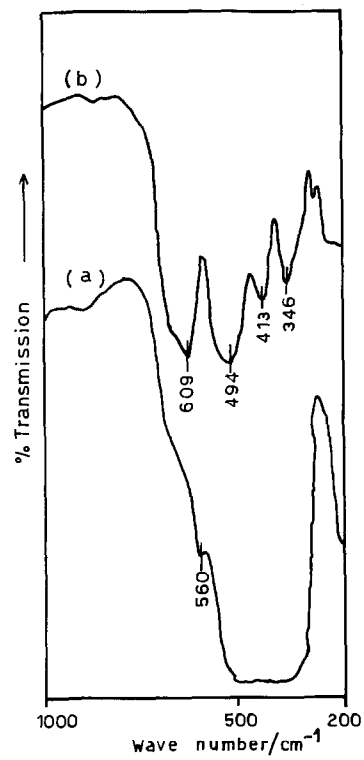

Fig. 5. Two IR spectra for the solid decomposition products of manganese acetate after heating to 400°C: (a) in N_2 and (b) in O_2.

3.3. X-ray diffraction analysis

Figure 6 shows seven X-ray diffractograms of the parent manganese acetate tetrahydrate (a) and its solid decomposition products at different temperatures (in different atmospheres).

Diffractogram (b) (at 125°C, N_2) and (c) (at 150°C, N_2) are identical which suggests the formation of an intermediate within that temperature range. On heating to 250°C in N_2 (diffractogram (d)), an unidentified new pattern is obtained which is different from patterns (b) and (c). This suggests, again, the formation of a second reaction intermediate.

Diffractograms (e), at 330°C, and (f), at 400°C in N_2, are similar and match well with ASTM standard data for MnO (ASTM card no. 7-230). Heating to 400°C in H_2 atmosphere gave the same MnO pattern as that obtained in N_2 atmosphere.

The solid decomposition product in O_2 atmosphere (diffractogram (g)), however, gave a different oxide, the pattern of which matches well with that of Mn_3O_4 (ASTM card no. 1-1127).

The X-ray results are in accordance with the IR results which suggest the formation of acetyl manganese acetate at 125°C. The IR results also suggest the

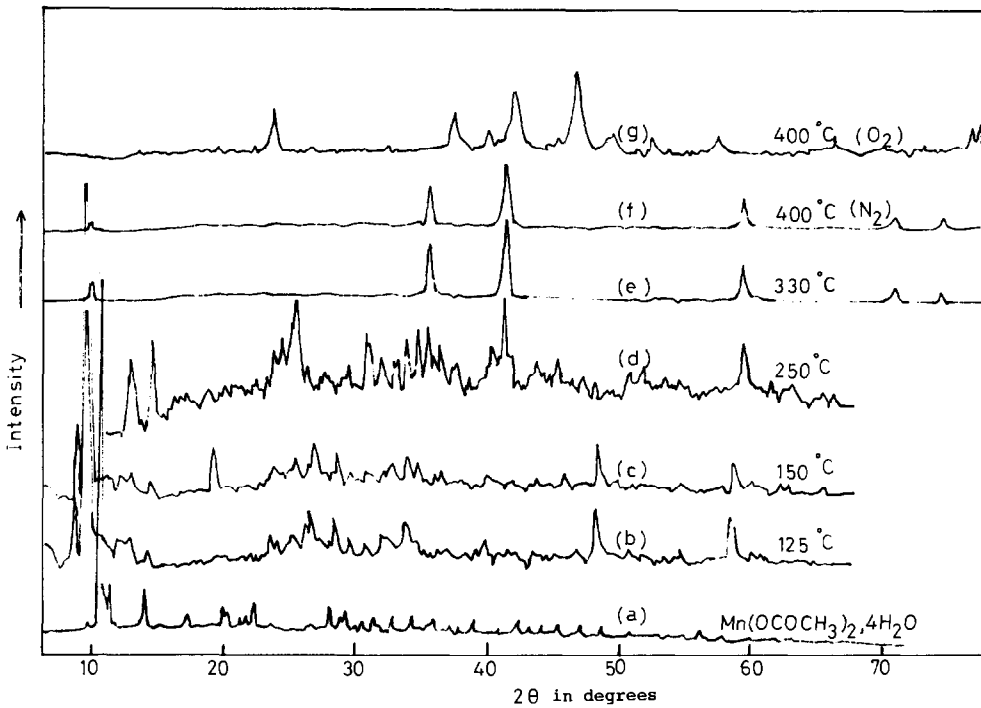

Fig. 6. X-ray diffractograms of the parent manganese acetate (a) and its solid decomposition products in N_2 at the temperatures: (b) 125°C, (c) 150°C, (d) 250°C, (e) 330°C, (f) 400°C and the product of heating at 400°C in O_2 (g).

formation of a second reaction intermediate, i.e. manganese acetate hydroxide, $Mn(CH_3COO)_2 \cdot OH$.

3.4. Gas-phase products

Gas chromatographic analysis of the volatile decomposition products in N_2 (and in O_2) atmospheres at different temperatures were carried out. In N_2 atmosphere, the volatile products at low temperature (≈ 100°C) were identified as acetic acid, acetone and traces of acetaldehyde. The proportion of acetaldehyde appreciably increases at 150°C and above.

At 270°C, two other products, CO_2 and CO, were detected in appreciable proportions. At 290°C, methane, isobutene and other unidentified products were also detected. The formation of methane and isobutene is thought to result from a bimolecular surface reaction involving the initially formed acetone [25, 26]

$$(CH_3)_2CO(s) + OH^-(s) + (CH_3)_2CO \rightarrow (CH_3)_2C{=}CH_2 + CH_3COO^-$$

$$(CH_3)_2CO + OH^-(s) \rightarrow CH_4 + CH_3COO^-(s)$$

The above two equations produce acetate surface species, supporting the IR results in which acetate species were shown to be present above 260°C, see Fig. 4.

This was proved experimentally when acetone vapour was passed over freshly prepared MnO (by heating the parent manganese acetate tetrahydrate to 400°C in N_2). The results showed that methane and isobutene were formed at the expense of acetone.

In the presence of oxygen, almost the same products were detected as in N_2 but acetone was the main product.

3.5. Scanning electron microscopy (SEM)

Figure 7 shows five representative micrographs (a)–(e) taken at different stages of the reaction.

Micrograph (a) shows that some crystallites of the parent salt have an irregular shape. Some broken parts appear on the surface of the crystallites indicating an early dehydration (thermal analysis results showed that dehydration starts at $\simeq 20$°C).

Micrograph (b) shows a sample that was heated at 125°C. It is clear that dehydration has taken place concurrently with melting. This supports our visual observations (using a simple melting-point apparatus) that the reactant melts at 120°C.

On heating to 150°C (micrograph (c)), a new type of crystallite appears, characterized by smooth, flat surfaces. This supports the DTA and DSC results (Figs. 2 and 3) where an exothermic process takes place in this temperature range, attributed to the formation of manganese acetate hydroxide intermediate, see IR results (Fig. 4).

Micrograph (d) shows a sample that was heated at 260°C. The features shown here are characteristic of melting, with wavy cracks and rounded pores [17].

Finally, micrograph (e) represents the residual solid product after heating (in N_2) at 400°C. It shows massive aggregates of small particles of the product MnO.

3.6. The decomposition course of $Mn(CH_3COO)_2 \cdot 4H_2O$

The thermal decomposition course of this salt can be summarized as follows.

(i) The dehydration process takes place in two steps between 20 and 125°C (endotherms **I** and **II**). The second step is accompanied by melting. At the end of the dehydration steps, an intermediate compound (acetyl manganese acetate) is formed (identified by IR, see Fig. 4).

(ii) A second reaction intermediate, i.e. manganese acetate hydroxide, is formed in an exothermic process near 150°C (exotherm **III**, Figs. 2 and 3), see the IR, XRD and GC results. This can be explained as

$$Mn(CH_3COO)_2COCH_3 \xrightarrow{H \cdot OH} CH_3CHO + Mn(CH_3COO)_2 \cdot OH$$

Acetaldehyde was identified by GC in appreciable amounts at 150°C and above, and the hydroxide compound was identified by IR spectroscopy.

(iii) MnO begins to form as a result of the decomposition of the acetate hydroxide intermediate in N_2 and in H_2 atmospheres (endotherm **IV**). In air, however, Mn_3O_4 is identified as the solid product.

(iv) Finally, a catalytic gas-phase reaction takes place on the surface of MnO, involving the initial gaseous products and acetate anions (endotherm **V**).

(a)

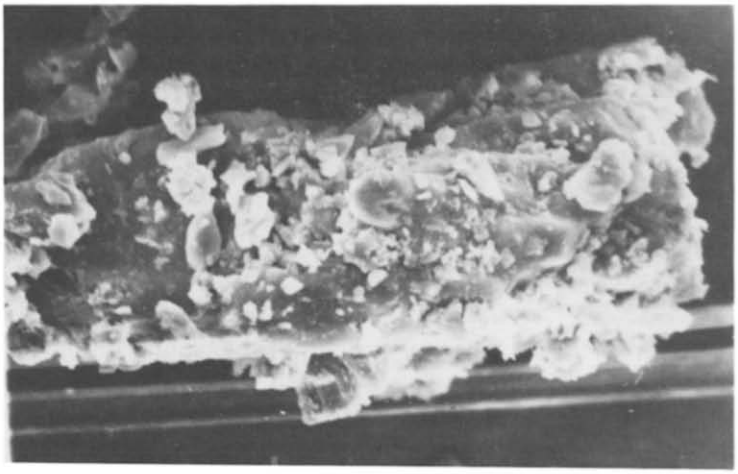

(b)

(c)

Fig. 1. (a)–(c)

(d)

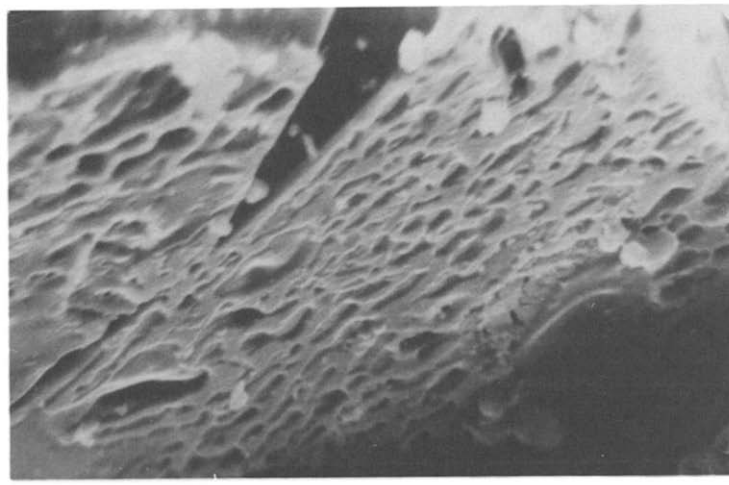

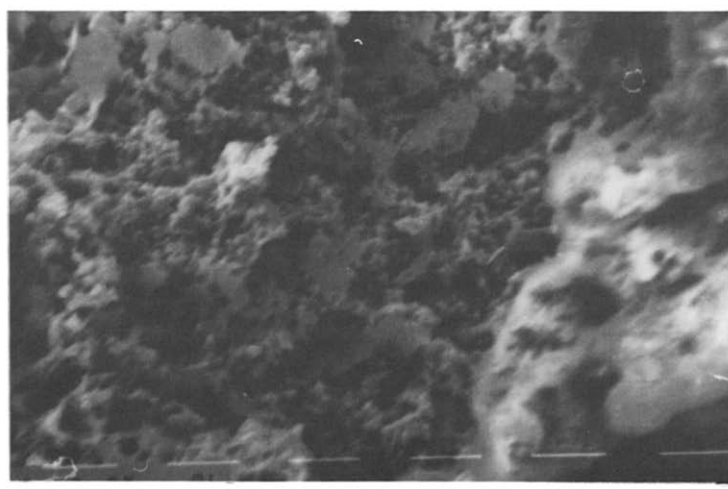

(e)

Fig. 7. Representative scanning electron micrographs of: (a) the parent salt (original magnification ×350); (b) sample heated at 125°C (original magnification ×500); (c) sample heated at 150°C (original magnification ×1000); (d) sample heated at 260°C (original magnification ×750); and (e) solid product on heating at 400°C in N_2 (original magnification ×1500).

4. Conclusions

The decomposition of manganese(II) acetate tetrahydrate shows a great deal of similarity to that of cobalt acetate tetrahydrate [11]. Both salts form the same type of intermediates, i.e. acetyl acetate and acetate hydroxide. The MnO, formed in N_2 and H_2, possesses catalytic activity, in that methane and isobutene were only

detected when this oxide started to be formed at ≈290°C. This is also similar to the behaviour of cobalt [11] and nickel [8] acetates which produce the corresponding active oxides. This was not the case for lead acetate where the PbO produced was not catalytically active [10].

The activation energy values reported here, Table 1, and the thermodynamic parameters, Table 2, are close to those reported for cobalt acetate [11].

We believe that low rates of heating, $\leq 10°C\ min^{-1}$ are useful in detecting and separating those processes which can be obscured on heating at high heating rates: exotherm **III** observed in the present study was not reported in the previous study by Diefallah [13], because of the high rate of heating ($15°C\ min^{-1}$) used.

The use of complementary analytical techniques, IR, X-ray diffraction and scanning electron microscopy, are useful for detecting reaction intermediates that have not been reported before and to determine the possibility of melt formation during the decomposition.

Mn_3O_4 is identified here as a solid product in air (by IR and X-ray diffraction), rather than Mn_2O_3 which was reported in other studies [13].

References

[1] M.E. Brown, D. Dollimore and A.K. Galwey, Reactions in the Solid State, Comprehensive Chemical Kinetics, Vol. 22, Elsevier, Amsterdam, 1980.
[2] M.A. Mohamed and A.K. Galwey, Thermochim. Acta, 217 (1993) 263.
[3] D.A. Dominey, H. Morley and D.A. Young, Trans. Faraday Soc., 61 (1965) 1246.
[4] M.A. Mohamed and A.K. Galwey, Thermochim. Acta, 213 (1993) 269.
[5] A.K. Galwey and M.A. Mohamed, Thermochim. Acta, 213 (1993) 279.
[6] D.L. Trimm, Design of Industrial Catalysts, Chemical Engineering Monograph II, Elsevier, Amsterdam, 1980.
[7] A.K. Galwey, S.G. McKee, T.R.B. Mitchell, M.E. Brown and A.F. Bean, Reactivity of Solids, 6 (1988) 173.
[8] M.A. Mohamed, S.A. Halawy and M.M. Ebrahim, J. Anal. Appl. Pyrol., 27 (1993) 109.
[9] R. Leibold and F. Huber, J. Therm. Anal., 18 (1980) 493.
[10] M.A. Mohamed, S.A. Halawy and M.M. Ebrahim, Thermochim. Acta, 236 (1994) 249.
[11] M.A. Mohamed, S.A. Halawy and M.M. Ebrahim, J. Therm. Anal., 41 (1994) 387.
[12] S.A.A. Mansour, G.A.M. Hussein and M.I. Zaki, Reactivity of Solids, 8 (1990) 197.
[13] E.M. Diefallah, Thermochim. Acta, 202 (1992) 1.
[14] C.P. Prabhakaran and S. Sarasukutty, Thermochim. Acta, 82 (1984) 391.
[15] M.A. Mohamed and S.A. Halawy, J. Therm. Anal., 41 (1994) 147.
[16] R.C. Weast (Ed.), Handbook of Chemistry and Physics, CRC press, Florida, 62nd edn., 1982.
[17] A.K. Galwey and M.A. Mohamed, Proc. R. Soc. London Ser. A, 396 (1984) 425.
[18] H.E. Kissinger, J. Anal. Chem., 29 (1957) 1702.
[19] A.W. Coats and J.P. Redfern, Nature, 201 (1964) 68.
[20] P. Baraldi and G. Fabbri, Spectrochim. Acta, 37 (1981) 89.
[21] R.L. Pecsok, L. Shields, T. Cairns and T.G. McWilliam, Modern Methods of Chemical Analysis, J. Wiley, London, 2nd edn., 1976.
[22] K.C. Patil, G.V. Chandrashekhar, M.V. George and C.N.R. Rao, Canadian J. Chem., 46 (1968) 257.
[23] K. Nakamoto, Infrared Spectra of Inorganic and Coordination Compounds, J. Wiley, London, 1963.
[24] A.K.H. Nohman, M.I. Zaki, S.A.A. Mansour, R.B. Fahim and C. Kappenstein, Thermochim. Acta, 210 (1992) 103.
[25] M.I. Zaki and N. Sheppard, J. Catal., 80 (1983) 114.
[26] A.V. Kiselev and A.V. Uvarov, Surf. Sci., 6 (1967) 399.